

# Self-synchronized Rectifier with Phase Information Extracted from Vibration Energy Harvester

Hang Yin and Takeaki Yajima\*

Department of Electrical and Electronic Engineering, Kyushu University,  
744 Motoooka, Nishi-ku, Fukuoka 819-0395, Japan

(Received February 4, 2022; accepted February 21, 2022)

**Keywords:** rectification, vibration energy, energy harvesting, passive circuit, low voltage

Low-loss rectification is essential for vibration energy harvesters. However, an extremely low loss is difficult to achieve in rectification using diodes due to the voltage drop caused by the threshold voltage of the diodes. Although synchronous rectification using transistors can avoid the voltage drop, it requires active control of the transistor gates. In this study, we achieved self-synchronized rectification using only passive elements by switching the transistors by separately extracting the phase information from a vibration energy harvester. The operation of the self-synchronized rectifier was demonstrated through simulations and experiments and was compared with that of a diode bridge. In addition, it was clarified that the self-synchronized rectifier is limited by the through current generated between the output terminals during switching and that the through current determines the lower limit of the power that can be rectified by this circuit. These results demonstrate a typical example where the performance trade-off of a power circuit can be addressed by co-designing the harvester device and the power circuit.

## 1. Introduction

Energy harvesting is expected to be a semi-permanent power source for next-generation edge devices used in anomaly detection, monitoring, telemetry, and other applications.<sup>(1)</sup> Among the various energy-harvesting technologies, vibration energy harvesters have been attracting attention because they can generate power without light or heat flow.<sup>(2)</sup> Because vibration energy harvesters generate AC power, rectification is required. In particular, since the power obtained from environmental vibration is small, low-loss rectification is indispensable.

The most common method of rectification is to use diodes such as a diode bridge circuit.<sup>(3–5)</sup> Since diodes are passive elements and do not require any control, a diode bridge circuit is an essential circuit for cold-start circuits before the power supply is turned on. However, it has the disadvantage of nontrivial power loss because a voltage drop due to the threshold voltage of the diode always occurs. On the other hand, synchronous rectification, in which the transistors are switched in synchronization with the mechanical vibration, avoids the voltage drop and thus

---

\*Corresponding author: e-mail: yajima@ed.kyushu-u.ac.jp

enables rectification with low power loss.<sup>(6–12)</sup> However, it usually requires active control to switch the transistors. To accurately switch the transistors on and off, it is necessary to detect the timing when the sign of the generated current reverses, and a zero-current detection circuit is often utilized.<sup>(6)</sup> In the zero-current detection circuit, a resistive element is inserted in the current path, and the voltages at both ends are compared to evaluate the current. However, both the resistive element and the comparator circuit consume extra power. In particular, if we try to generate a high voltage near the zero current to improve sensitivity, a large voltage loss occurs near the current peak. Furthermore, since the current amplitude obtained from the environment varies by orders of magnitude with time, high sensitivity in small-power generation will inevitably result in large Joule losses when the amount of power generation is large. This trade-off can be partially eliminated by using a high-speed, high-accuracy comparator. In that case, however, the power consumption of the comparator will increase and cancel the small power obtained from the environmental vibration. Therefore, for low-loss synchronous rectification, the essential issue is how to detect the exact timing of current sign reversal with low power consumption.

Several solutions for synchronous rectification have been proposed in fields different from energy harvesting. For example, in DC–DC converters, the phase information can be extracted directly from the magnetic flux by adding an extra winding to the inductor and used for synchronous rectification.<sup>(7,8)</sup> In wireless power transfer, a synchronous rectifier circuit has been constructed by detecting the peak of the capacitive voltage or by using the voltage in a resonant filter.<sup>(9,10)</sup> Adaptive control was also proposed to be suitable for wireless power transfer because it can avoid the difficulties inherent to high frequencies.<sup>(11,12)</sup> However, these methods cannot simply be applied to vibration energy harvesters because of the significant limitations in terms of power consumption, size, and power fluctuation. Although the cross-coupling topology of metal-oxide-semiconductor field-effect transistor (MOSFET) bridges can partially mitigate this problem,<sup>(13,14)</sup> it suffers from severe backward current when the input voltage becomes low.

In this study, we solved this problem by directly extracting the phase of the vibration from a vibration energy harvester as shown in Fig. 1. A mechanically integrated but electrically isolated

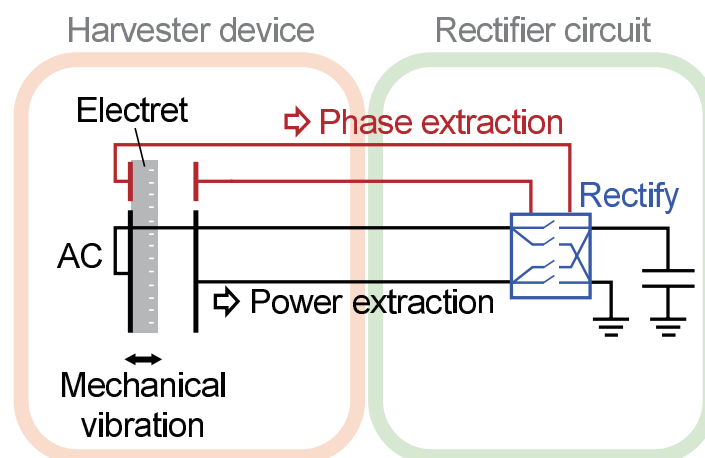


Fig. 1. (Color online) Schematic illustration of a self-synchronized rectifier that performs rectification by extracting the phase information from the vibration energy harvester. In this way, low-loss rectification is possible using only passive elements.

phase signal extraction part is provided in the harvester device, and the generated power can be rectified on the basis of the extracted phase signal. The self-synchronized rectifier was demonstrated by simulation as well as by experiments using a prototype chip. It was also shown that a through-current path is generated in the self-synchronized rectifier during switching, which determines the lower limit of the power that can be rectified. The low-loss rectification using only passive elements by co-designing the harvester device and the power circuit is expected to be a useful technology for next-generation edge devices.

## 2. Model

In this study, we focused on electrets or piezoelectric vibration energy harvesters. Both of them have higher impedance than other types of energy harvesters and can be approximated by a parallel circuit of the current source and the capacitor in a practical voltage range. As mentioned earlier, the self-synchronized rectifier is realized by adding a phase extraction part to the vibration energy harvester. This can be easily achieved by electrically separating the phase extraction part and the harvester device while keeping them mechanically in one piece. Let  $r$  be the area ratio of the phase extraction part to the power extraction part. As shown in Fig. 1, the current and capacitance of the phase extractor are both  $r$  times those in the power extraction part. The current from the phase extraction part is converted by the diode into a voltage signal that reverses in synchronization with the mechanical vibration. Therefore, if this voltage is used to drive the gate of the transistor in the rectifier circuit, the current output from the power extraction part can be rectified. If we define the efficiency as the ratio of the output power to the input power, the efficiency of the self-synchronized rectifier is ideally unity. As a comparison, the efficiency of a diode bridge circuit is  $V_{OUT} / (V_{OUT} + 2V_D)$ , where the voltage drop per diode is  $V_D$  and the output voltage is  $V_{OUT}$ .

## 3. Materials and Methods

In this study, a self-synchronized rectifier circuit using the phase information from the harvester device was demonstrated by simulation and experiments. We also performed the simulation on a diode bridge for comparison to clarify the features of the self-synchronized rectifier. In a harvester device using an electret, the capacitance is relatively small (on the order of 100 pF) because the distance between the electrodes is large. On the other hand, in a piezoelectric vibration energy harvester, the capacitance is larger because of the small inter-electrode distance and the large permittivity of the piezoelectric material. In this study, the capacitance of the generating element was set to 200 pF unless specified, and the operation of the circuit was verified by varying the current amplitude ( $I_0$ ) from 1  $\mu$ A to 1 mA.

The self-synchronized rectifier has two sets of input terminals: one for power extraction and the other for phase extraction, as shown in Fig. 2(a). These terminals are connected to the power extraction and phase extraction parts of the harvester device, respectively. In the experiments, the harvester device was reproduced by two synchronized AC current sources (Keithley 6221) with appropriate parallel capacitances. Unless otherwise stated, the current ratio of the power

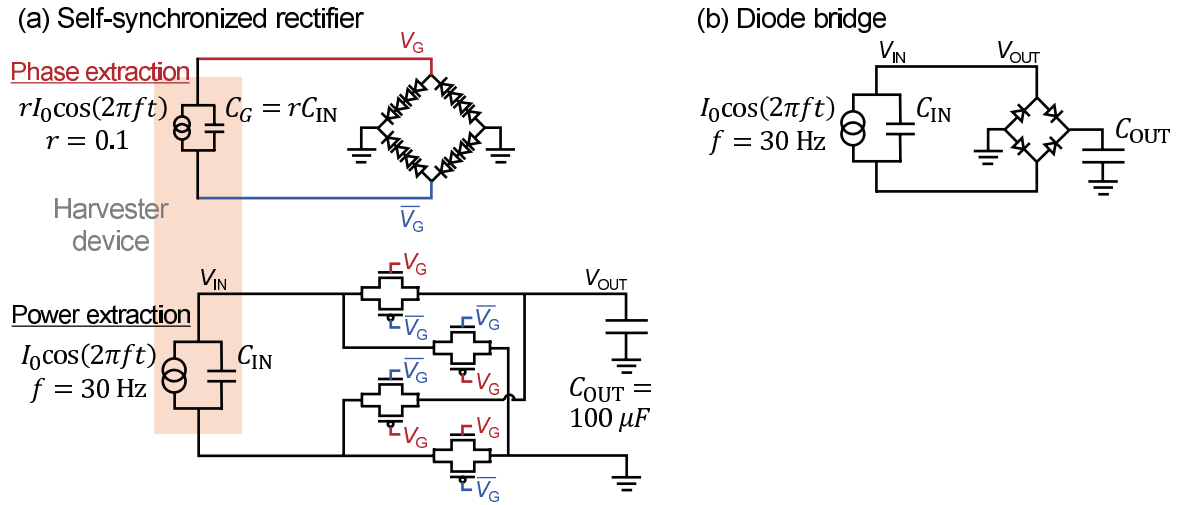


Fig. 2. (Color online) (a) Circuit diagram of the self-synchronized rectifier. The harvester device (orange shadow) is approximated by an AC current source and a capacitor, and the area ratio of the phase extraction part to the power extraction section is denoted as  $r$ . The phase signals  $V_G$  and  $\bar{V}_G$  generated by the phase extraction part are used to rectify the generated AC power. (b) Circuit diagram of the diode bridge circuit for comparison

extraction part to the phase extraction part was set to  $r = 0.1$ . Since the total parasitic capacitance of the Keithley 6221 current sources and wiring was approximately 20 pF, a 180 pF ceramic capacitor was added to achieve a total capacitance of 200 pF for the power extraction part. For the phase extraction part, only a parasitic capacitance of 20 pF was used. As a result, the capacitance ratio was also set to  $r = 0.1$ .

Figure 2 shows the circuit diagrams of the self-synchronized rectifier circuit and the diode bridge circuit used in this study. In the self-synchronized rectifier circuit, the current input from the phase extractor is converted into voltage signals ( $V_G$  and  $\bar{V}_G$ ) by diodes made of high-threshold p-MOSFETs. These diodes have two roles: one is to convert a small amount of current into a large voltage signal, and the other is to clamp the voltage against the phase extraction current. Here, voltage clamping is necessary because the phase extraction part typically generates a current amplitude larger than sub- $\mu\text{A}$ , and then, its 20 pF capacitance leads to an excessive open-circuit voltage larger than 50 V. The positive and negative switching of the voltages generated in these diodes roughly corresponds to the timing when the charging current becomes zero, and these voltages can be directly used to drive the gate of the rectifier circuit.

A p-MOSFET and n-MOSFET pair in parallel was used as the rectifier transistor so that no voltage drop occurs irrespective of the output voltage ( $V_{OUT}$ ). Simulations and experiments were performed using the Taiwan Semiconductor Manufacturing Company (TSMC) 180 nm process. The diodes in the diode bridge circuit were low-threshold Schottky barrier diodes (SBDs) provided by TSMC to minimize the voltage drop. The voltage drop per diode ( $V_D$ ) is about 0.2 V at 10  $\mu\text{A}$  current and about 0.4 V at 1 mA. The efficiency of the rectifier circuit was calculated from the ratio of output power ( $P_{OUT}$ ) to input power ( $P_{IN}$ ), averaged for one oscillation period when the capacitor on the output side was charged to 1 V.

## 4. Results

Figure 3(a) shows the  $V_{OUT}$  waveform obtained from the simulation of the self-synchronized rectifier. It can be seen that the input current is rectified and the output capacitor is charged. The magnified waveforms of the input voltage ( $V_{IN}$ ),  $V_{OUT}$ , and  $V_G$  are shown in Fig. 3(b). The voltage drop between  $V_{IN}$  and  $V_{OUT}$  is small enough to suppress the power loss. This is in contrast to the case of the diode bridge circuit in Fig. 3(c), for which  $V_{OUT}$  drops by  $2V_D$  with respect to  $V_{IN}$ , indicating a large power loss in rectification.

Figure 4(a) shows an optical micrograph of the prototype chip of the self-synchronized rectifier, and Figs. 4(b) and 4(c) show the measured waveforms of  $V_{IN}$  and  $V_{OUT}$ . It can be seen that the voltage drop in the self-synchronized rectifier is also small in the measured data. Thus, the self-synchronized rectifier circuit enables low-loss rectification with a small voltage drop.

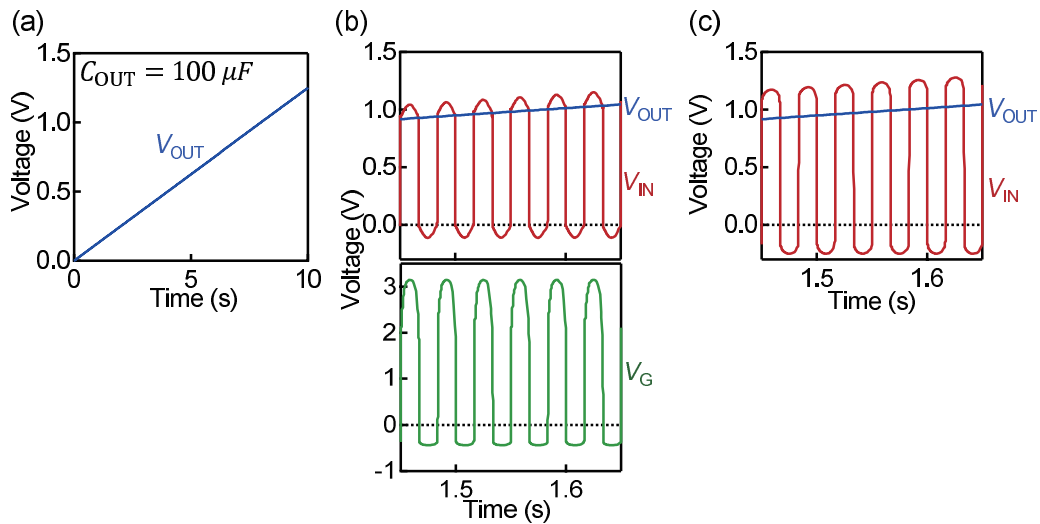


Fig. 3. (Color online) (a) Simulation of  $V_{OUT}$  for  $I_0 = 100 \mu\text{A}$  and  $C_{OUT} = 100 \mu\text{F}$  in the self-synchronized rectifier. (b) Magnified view of simulated  $V_{IN}$ ,  $V_{OUT}$ , and  $V_G$ , showing that the voltage drop is small. (c) Simulated  $V_{IN}$  and  $V_{OUT}$  of the diode bridge circuit, where the voltage drop is larger than that of the self-synchronized rectifier circuit in (b).

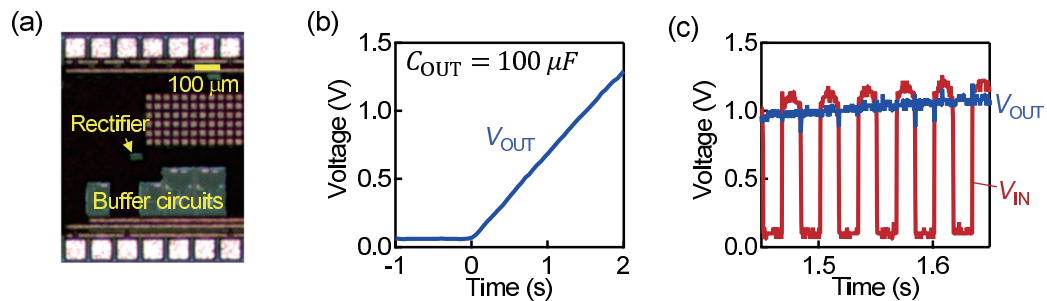


Fig. 4. (Color online) (a) Optical micrograph of the prototype chip of the self-synchronized rectifier circuit. The circuit itself is as small as  $950 \mu\text{m}^2$ , and most of the other area is occupied by the buffer circuit and the electrode pads. (b) Measured  $V_{OUT}$  of the self-synchronized rectifier circuit. (c) Magnified view of measured  $V_{IN}$  and  $V_{OUT}$ , both observed through buffer circuits using amplifiers so that the measurement does not affect the circuit operation.

Figure 5(a) summarizes the efficiency of the self-synchronized rectifier circuit and the diode bridge circuit obtained from the simulation and experiments plotted against the output power. It can be seen that the overall efficiency of the self-synchronized rectifier is higher than that of the diode bridge. The higher efficiency can be attributed to the reduced voltage drop in the self-synchronized rectifier. On the other hand, the efficiency of the self-synchronized rectifier gradually decreases for larger  $P_{OUT}$  because  $V_{IN}$  is large enough to incur a voltage drop at the switch transistor. This problem can be solved by increasing the width of the switch transistor to achieve a higher ON current.

The efficiency of the self-synchronized rectifier circuit drops for smaller  $P_{OUT}$ , especially in the experiment, because of the through-current flow between the output terminals during switching as shown in Fig. 5(b) (orange and green lines). The through-current paths are shown in Fig. 5(c), and it can be seen that the complementary metal-oxide-semiconductor (CMOS) structure inherently exists inside the switching circuit, and through current flows every time  $V_G$  and  $\bar{V}_G$  take an intermediate value. The effect of this through current can be clearly confirmed by experiments. Figure 5(d) shows the waveform of  $V_{OUT}$  at  $I_0 = 5 \mu\text{A}$  when the output capacitor ( $C_{OUT}$ ) was intentionally made as small as 89 nF. It can be seen that a through current flows at each switching and prevents  $V_{OUT}$  from increasing. This through current is the main factor reducing the efficiency of the self-synchronized rectifier circuit for small  $P_{OUT}$ . Indeed, when the generated current in the harvester is below this value on average,  $V_{OUT}$  becomes saturated and the rectification stops. One of the characteristics of this through current is that its magnitude is extremely sensitive to the steepness and timing difference of  $V_G$  and  $\bar{V}_G$ . In fact, the

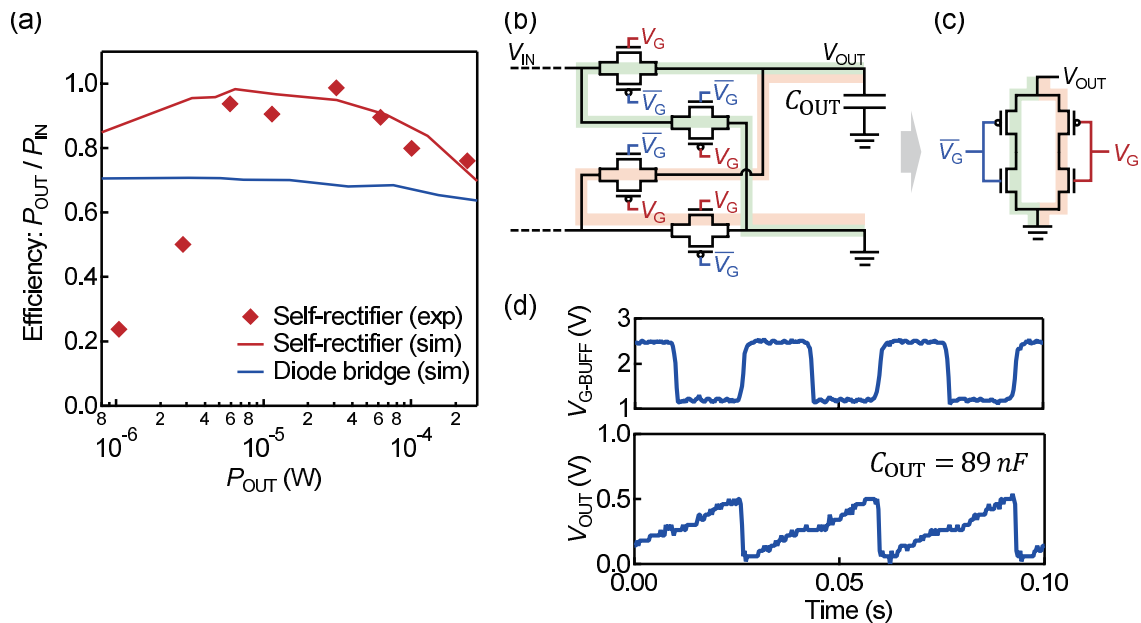


Fig. 5. (Color online) (a) Efficiency of the self-synchronized rectifier circuit and the diode bridge circuit with respect to  $P_{OUT}$ . Marks represent measured values (“exp”) and curves represent the simulation results (“sim”). It can be seen that the self-synchronized rectifier is generally more efficient than the diode bridge circuit. (b) Two through-current paths (orange and green) generated in the self-synchronized rectifier during switching. (c) CMOS structures of the two through-current paths. (d) Experimental  $V_{OUT}$  waveform showing the effect of through current.  $V_{G-BUFF}$  denotes the voltage converted from  $V_G$  through the inverting buffer circuit, where  $V_{G-BUFF} = 2.5 \text{ V}$  corresponds to  $V_G = 0 \text{ V}$ .

experimental data in Fig. 5(d) shows that the magnitude of the through current is markedly different between the rise and fall of  $V_{G-BUFF}$ , whereas ideally it should be symmetrical. Furthermore, the effect of the through current was also different between the experiments and the simulation. The experiments showed a larger effect of the through current, and hence, a narrower operation window of  $P_{OUT}$ . From these analyses, the reduced efficiency at  $P_{OUT}$  is because the steepness of  $V_G$  and  $\bar{V}_G$  is lost for smaller current amplitudes and the through current increased. This is a limitation of self-synchronized rectification using only passive elements, and if we want to rectify the power to low  $P_{OUT}$  with high efficiency, we need to shift the switching timing by active control to prevent the through current.

Figure 6(a) shows the frequency dependence of the efficiency of the self-synchronized rectifier and the diode bridge circuit. The measured values are in good agreement with the simulations, and it can be seen that the efficiency hardly decreases in the range of several Hz to several kHz, which is generally used in vibration energy harvesters.

Figure 6(b) shows the characteristics of the self-synchronized rectifier when the area ratio  $r$  is changed from 0.1 to 0.5. It can be seen that the efficiency is not largely affected by  $r$  as long as the same  $r$  value is used between the current and the capacitance. From the mechanical viewpoint, if  $r$  is increased, the volume of the harvester device will be increased by an extra volume of the phase extraction part. Therefore, it is preferable to make  $r$  smaller. On the other hand, if  $r$  is made too small, the parasitic capacitance in the wiring becomes non-negligible and the capacitance ratio deviates from the designed value of  $r$ .

Note that if the capacitance ratio between the power extractor and the phase extractor deviates from the designed value  $r$ , the accuracy of the extracted phase deteriorates and the efficiency decreases. Figure 6(c) shows the simulation results when the current ratio is set to  $r = 0.1$  and the capacitance of the phase extraction part ( $C_G$ ) is varied with a fixed capacitance of the power extraction part ( $C_{IN} = 200$  pF). The efficiency is maximum when  $C_G = 20$  pF, where the capacitance ratio matches the current ratio  $r = 0.1$ . As shown in Fig. 6(c), this effect is critical when the generation current is small ( $1 \mu\text{A}$ ) because charging the capacitance takes time and the resultant large phase shift lowers the efficiency.

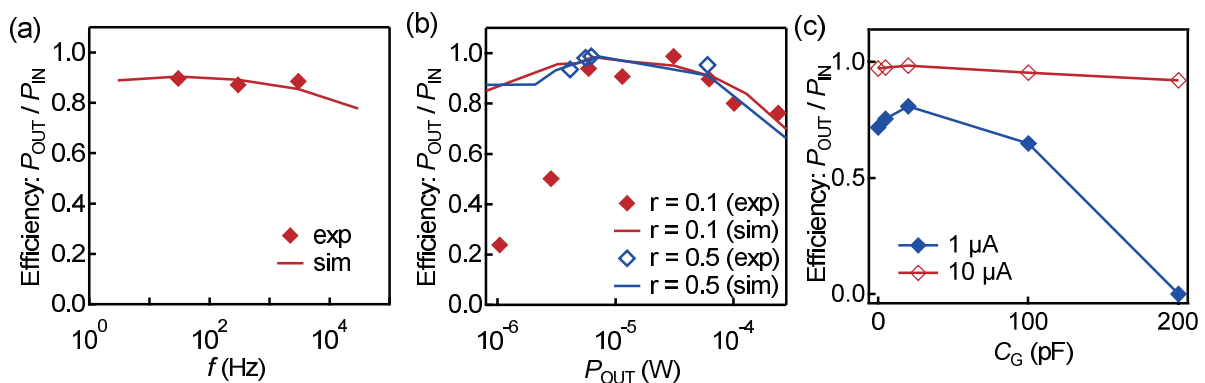


Fig. 6. (Color online) (a) Effect of vibration frequency  $f$  on the efficiency of the self-synchronized rectifier. (b) Comparison of the efficiency of the self-synchronized rectifier at  $r = 0.1$  and  $0.5$ . (c) Simulation results of the efficiency of the self-synchronized rectifier circuit.  $r$  and  $C_{IN}$  are fixed to  $0.1$  and  $200$  pF, respectively, and  $C_G$  is varied. When  $r = C_G / C_{IN}$ , the phase shift is eliminated and the efficiency is maximized.

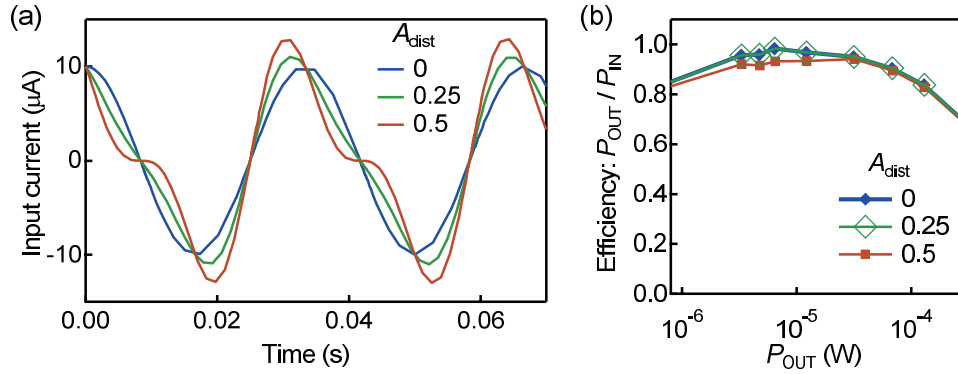


Fig. 7. (Color online) (a) Waveforms of the input current for the power extraction part, used in simulating the effect of waveform distortion. Here, using the distortion parameter  $A_{dist}$ , we expressed the distorted current waveform as  $I_0[\cos(2\pi ft) - A_{dist}\cos(4\pi ft)]$ , for example. The drawing corresponds to the data for  $I_0 = 10 \mu\text{A}$ . In the simulation, one-tenth of this current is input to the phase extraction part. (b) Simulation results for the efficiency of the self-synchronized rectifier circuit when  $A_{dist}$  is varied from 0 to 0.5.

Finally, we discuss the effect of waveform distortion from an ideal sinusoidal curve. In electret vibration energy harvesters, the current waveform from the harvester device is often distorted.<sup>(15,16)</sup> To evaluate the effect of this distortion on the efficiency of the self-synchronized rectifier, a simulation was performed by assuming the generated current is  $I_0[\cos(2\pi ft) - A_{dist}\cos(4\pi ft)]$  instead of  $I_0\cos(2\pi ft)$  in Fig. 2(a). Here,  $A_{dist}$  is a parameter that represents the magnitude of distortion as shown in Fig. 7(a). We input one-tenth of this current to the phase extractor ( $r = 0.1$ ) and obtained the efficiency of the self-synchronized rectifier circuit as shown in Fig. 7(b). It can be seen that the distortion parameter  $A_{dist}$  has no significant effect on the efficiency.

## 5. Conclusion

In this study, we have achieved low-loss self-synchronized rectification using only passive elements by separately extracting the phase information of the vibration energy harvester. This self-synchronized rectifier can achieve highly efficient rectification and can also be used in a cold start without a power supply. On the other hand, as a trade-off of the passive operation, there is a problem of through current during switching, which has a significant impact, especially at low generated power. Thus, the co-design of the harvester device and the power circuit makes it possible to simplify the design of the entire system and increase efficiency, but at the same time, it causes different trade-offs that should be taken into account. This study provides an essential example for the co-design of the device and the circuit as an important guideline for constructing energy-harvesting systems.

## Acknowledgments

We would like to express our deepest gratitude to Dr. Izumi Hayashibara and Dr. Hiroshi Matsumoto of The University of Tokyo for their support in the circuit design. For fabrication, we

would like to express our deepest appreciation to VDEC, The University of Tokyo, in collaboration with Cadence Design Systems, and DISCO Corporation. We thank Prof. Hiroshi Toshiyoshi and Prof. Hiroaki Honma of The University of Tokyo and Dr. Hiroyuki Mitsuya of Saginomiya Seisakusho, Inc., for the discussion on vibration energy harvesters. This work was supported by the Japan Science and Technology Agency (Grant No. JPMJCR21Q2).

## References

- 1 S. Sudevalayam and P. Kulkarni: IEEE Commun. Surv. Tut. **13** (2011) 443. <https://doi.org/10.1109/SURV.2011.060710.00094>
- 2 S. P. Beeby, M. J. Tudor, and N. M. White: Meas. Sci. Technol. **17** (2006) R175. <https://doi.org/10.1088/0957-0233/17/12/R01>
- 3 E. Lefeuvre, D. Audigier, C. Richard, and D. Guyomar: IEEE Trans. Pow. Electron. **22** (2007) 2018. <https://doi.org/10.1109/TPEL.2007.904230>
- 4 K. Makihara, S. Takeuchi, S. Shimose, and J. Onoda: Trans. JSASS Aerospace Tech. Jpn. **10** (2012) Pc\_13. [https://doi.org/10.2322/tastj.10.Pc\\_13](https://doi.org/10.2322/tastj.10.Pc_13)
- 5 S. Faghihi and M. Moallem: IEEE/ASME Int. Conf. Adv. Intel. Mech. (2012) 754. <https://doi.org/10.1109/AIM.https://doi.org/2014.6878169>
- 6 M. S. Amouzandeh, B. Mahdavihah, A. Prodic, and B. McDonald: Proc. IEEE Applied Power Electronics Conference and Exposition (APEC) (2016) 329. <https://doi.org/10.1109/APEC.2016.7467892>
- 7 I. D. Jitaru: APEC Seventeenth Annual IEEE Applied Power Electronics Conference and Exposition (2002) 867. <https://doi.org/10.1109/APEC.2002.989345>
- 8 H. Jia, O. Abdel-Rahman, K. Padmanabhan, P. Shea, I. Batarseh, and Z. J. Shen: Intelec **2010** (2010) 20.3. <https://doi.org/10.1109/INTLEC.2010.5525665>
- 9 M. Kim and J. Choi: IEEE Energy Conversion Congress and Exposition (ECCE) (2020) 4607. <https://doi.org/10.1109/ITEC48692.2020.9161711>
- 10 S. Mukherjee, V. P. Galigekere, and O. Onar: IEEE Transportation Electrification Conference and Expo (ITEC) (2020) 955. <https://doi.org/10.1109/INTLEC.2010.5525665>
- 11 C. Fei, Q. Li, and F. C. Lee: IEEE Trans. Pow. Electron. **33** (2018) 5351. <https://doi.org/10.1109/APEC.2016.7467891>
- 12 M. Zhou and H. Wang: IEEE Applied Power Electronics Conference and Exposition (APEC) (2020) 2073. <https://doi.org/10.1109/APEC39645.2020.9124005>
- 13 A. Romani, M. Filippi, M. Dini, and M. Tartagni: ACM J. Emerging Technol. Comput. Syst. **12** (2015) 1. <https://doi.org/10.1145/2700244>
- 14 J. Wang, A. J. Dancy, and D. S. Ha: IECON 2018 - 44th Annual Conference of the IEEE Industrial Electronics Society (2018) 1975. <https://doi.org/10.1109/IECON.2018.8591639>
- 15 K. Tao, J. Wu, L. Tang, L. Hu, S. W. Lye, and J. Miao: J. Micromech. Microeng. **27** (2017) 044002. <https://doi.org/10.1088/1361-6439/aa5e73>
- 16 Y. Zhang, T. Wang, A. Luo, Y. Hu, X. Li, and F. Wang: Appl. Energy **212** (2018) 362. <https://doi.org/10.1016/j.apenergy.2017.12.053>